The Journal of Immunology

RESEARCH ARTICLE | MARCH 15 2016

Splenic RNA and MicroRNA Mimics Promote Complement Factor B Production and Alternative Pathway Activation via Innate Immune Signaling

Lin Zou; ... et. al

J Immunol (2016) 196 (6): 2788–2798.
https://doi.org/10.4049/jimmunol.1502106

Related Content

Suppression of Experimental Autoimmune Encephalomyelitis Using Peptide Mimics of CD28

J Immunol (August,2002)

Development of a Lipopolysaccharide-Targeted Peptide Mimic Vaccine against Q Fever

J Immunol (November,2012)

A Mimic of $p21^{WAF1/CIP1}$ Ameliorates Murine Lupus

J Immunol (November,2005)

Downloaded from http://journals.aai.org/jimmunol/article-pdf/196/6/2788/1417822/1502106.pdf by guest on 06 March 2025

Splenic RNA and MicroRNA Mimics Promote Complement Factor B Production and Alternative Pathway Activation via Innate Immune Signaling

Lin Zou,*,† Yan Feng,*,† Ganqiong Xu,* Wenling Jian,* and Wei Chao*,†

Complement factor B (cfB) is an essential component of the alternative pathway (AP) and plays an important role in the pathogenesis of polymicrobial sepsis. However, the mechanism leading to cfB production and AP activation during sepsis remains poorly understood. In this study, we found that plasma cell–free RNA was significantly increased following cecal ligation and puncture (CLP), an animal model of polymicrobial sepsis, and was closely associated with sepsis severity. Quantitative RT-PCR and microRNA (miRNA) array analysis revealed an increase in bacterial RNA and multiple host miRNAs (miR-145, miR-146a, miR-122, miR-210) in the blood following CLP. Treatment with tissue RNA or synthetic miRNA mimics (miR-145, miR-146a, miR-122, miR-34a) induced a marked increase in cfB production in cardiomyocytes or macrophages. The newly synthesized cfB released into medium was biologically active because it participated in AP activation initiated by cobra venom factor. Genetic deletion of TLR7 or MyD88, but not TLR3, and inhibition of the MAPKs (JNK and p38) or NF-κB abolished miR-146a–induced cfB production. In vivo, CLP led to a significant increase in splenic cfB expression that correlated with the plasma RNA or miRNA levels. Peritoneal injection of RNA or miR-146a led to an increase in cfB expression in the peritoneal space that was attenuated in MyD88-knockout or TLR7-knockout mice, respectively. These findings demonstrate that host cellular RNA and specific miRNAs are released into the circulation during polymicrobial sepsis and may function as extracellular mediators capable of promoting cfB production and AP activation through specific TLR7 and MyD88 signaling. ***The Journal of Immunology*****, 2016, 196: 2788–2798.**

During sepsis, invading pathogens and endogenous molecules released from injured tissues interact with host cells and cause massive activation of innate immune responses, including immune cell activation, cytokine production, and complement system activation (1). Complement is a part of the innate immune system and functions against invading pathogens (2). It can also promote cytokine and reactive oxygen species production that ultimately leads to organ injury in severe sepsis (3–6). Complement factor B (cfB) is an essential component of the alternative pathway (AP) and amplifies complement activation (7). We recently reported that cfB is upregulated in serum and in major organs, including the heart and kidney, following cecal ligation and puncture (CLP) and may contribute to the pathogenesis of polymicrobial sepsis (3). Systemic cfB deficiency improves animal survival and cardiac function and attenuates acute kidney injury in severe sepsis. Moreover, other investigators demonstrated that locally synthesized, rather than serum, complements are of major importance in tissue injury (8–11). Although TLRs are known to regulate cfB production (3, 12), the mechanisms leading to the critical cfB upregulation and AP activation in severe sepsis remain incompletely understood.

During bacterial infection, nucleic acids are released into the extracellular space from invading pathogens and injured tissues (13). These include various types of RNA, such as tRNA, rRNA, mRNA, and microRNA (miRNA) (14). These extracellular RNAs may provoke inflammation and induce tissue injury. For example, in a sterile model of tissue injury, eliminating extracellular RNA by systemic delivery of RNase reduces myocardial inflammation and injury following a transient ischemia (15, 16). Extracellular RNA induces a potent inflammatory response of the cardiovascular system by enhancing leukocyte recruitment (15, 17) and cytokine production (15, 18).

miRNAs are a group of small noncoding RNAs. The primary role of miRNA is to regulate gene expression inside the cell at the posttranscriptional level by binding to the 3′ untranslated region of the target mRNAs. Thus, by affecting protein translation, miRNAs act as regulators (repressors) of a wide range of biological processes and play a dominant role in health and diseases (19–21). miRNA may also function as cell-to-cell communicators. miRNA can be actively secreted or passively released from cells (22) and in different pathological conditions, such as ischemia (15) and sepsis (14). miRNAs circulate in the blood in various forms, such as exosomes, microvesicles, high-density lipoprotein, and RNA-binding proteins, which protect them from RNase digestion; thus, they are highly stable in the blood. These miRNAs reportedly act on target cells and play an important role in the pathogenesis of diseases (23).

In the current study, we tested the hypothesis that endogenous tissue RNA, including various miRNAs, is released into the cir-

*Department of Anesthesia, Critical Care, and Pain Medicine, Massachusetts General Hospital, Harvard Medical School, Boston, MA 02114; and †Department of Anesthesiology, University of Maryland School of Medicine, Baltimore, MD 21201

Received for publication September 28, 2015. Accepted for publication January 6, 2016.

This work was supported in part by National Institutes of Health Grant GM097259 (to W.C.) and a mentored research award from the International Anesthesia Research Society (to L.Z.).

The sequences presented in this article have been submitted to the National Center for Biotechnology Information Gene Expression Omnibus under accession number GSE74952.

Address correspondence and reprint requests to Dr. Wei Chao, Department of Anesthesiology, University of Maryland School of Medicine, 22 South Greene Street S11C00, Baltimore, MD 21201. E-mail address: wchao@anes.umm.edu

Abbreviations used in this article: AP, alternative pathway; cfB, complement factor B; CLP, cecal ligation and puncture; CVF, cobra venom factor; miRNA, microRNA; poly(I:C), polyinosinic-polycytidylic acid; qRT-PCR, quantitative RT-PCR; WT, wild-type.

Copyright © 2016 by The American Association of Immunologists, Inc. 0022-1767/16/$30.00

Downloaded from http://journals.aai.org/jimmunol/article-pdf/196/6/2788/1417822/1502106.pdf by guest on 06 March 2025

culation during severe polymicrobial sepsis and that tissue RNA and miRNAs are capable of stimulating complement factor B production and AP activation through specific innate immune signaling.

Materials and Methods

Reagents

Abs against phospho-p38, phospho-ERK1/2, phospho-JNK, IκB-α, and GAPDH were purchased from Cell Signaling Technology (Beverly, MA). Total p38, ERK1/2, and JNK Abs were from Santa Cruz Biotechnology (Dallas, TX). Bovine pancreas RNase A, Lipofectamine 3000, TRIzol LS, SYTO RNASelect Green Fluorescent Cell Stain, and the Quant-iT RNA Assay Kit were from Invitrogen Life Technologies (Carlsbad, CA). The TLR ligands, polyinosinic-polycytidylic acid [poly(I:C)], Pam3Cys, and CpG, were from Enzo Life Sciences (Farmingdale, NY). DNase was from Thermo Scientific (Waltham, MA). Imiquimod (R837, TLR7 ligand) and CL075 (TLR7/8 ligand) were from InvivoGen (San Diego, CA). Human cfB Ab and cobra venom factor (CVF) were purchased from Complement Technology (Tyler, TX). TRIzol reagent used to extract RNA from cell or tissues and HRP-conjugated donkey anti-goat IgG were from Sigma-Aldrich (St. Louis, MO). Protease and phosphatase inhibitors were from Roche Diagnostics (Indianapolis, IN). miRNA mimics were synthesized by Integrated DNA Technologies (Coralville, IA); sequences are listed in Table I. The miScript II RT Kit, the miScript SYBR Green PCR Kit, and miRNA primers for quantitative RT-PCR (qRT-PCR) were purchased from QIAGEN (Valencia, CA). Criterion XT Bis-Tris Precast Gels were purchased from Bio-Rad (Hercules, CA). Luminata Forte Western HRP substrate was from Millipore (Billerica, MA).

Animals

Eight- to sixteen-week-old gender- and age-matched mice were used. C57BL/6J wild-type (WT), $TLR7^{-/-}$, and $TLR3^{-/-}$ mice were purchased from the Jackson Laboratory and housed in a Massachusetts General Hospital animal facility for ≥1 wk before experiments. $cfB^{-/-}$ mice were kindly provided by X. Wu (Washington University School of Medicine in St. Louis, St. Louis, MO). $MyD88^{-/-}$ mice were provided water supplemented with sulfamethoxazole (4 mg/ml) and trimethoprim (0.8 mg/ml). Antibiotics were stopped ≥2 wk prior to experiments. All animals were housed in pathogen-free, temperature-controlled, and air-conditioned facilities with 12-h/12-h light/dark cycles and fed with the same bacteria-free diet. All animal care and procedures were performed according to the protocols approved by the Subcommittee on Research Animal Care of Massachusetts General Hospital and were in compliance with the *Guide for the Care and Use of Laboratory Animals* published by the National Institutes of Health.

Mouse model of polymicrobial sepsis

A clinically relevant rodent model of sepsis was created by CLP, as described previously (3, 24, 25). In brief, mice were anesthetized, and the cecum was ligated 1.2 cm from the tip and punctured with an 18-gauge needle. A small amount of fecal material was squeezed out gently. The sham-operated mice underwent laparotomy but without CLP. After surgery, prewarmed normal saline (0.05 ml/g body weight) was administered s.c. Postoperative pain control was managed with s.c. injection of bupivacaine (3 mg/kg) and buprenorphine (0.1 mg/kg). Postoperatively, mice were monitored for rectal temperature and sepsis severity score (0 = bright, alert, and responsive; 1 = slightly lethargic; 2 = lethargic and hunched; 3 = very lethargic, hunched, and shaky; 4 = dead), as described previously (26).

miRNA array

Plasma was prepared from EDTA anticoagulated blood of sham and septic mice at 24 h after surgery. The profile of 68 miRNAs related to an immunology panel was analyzed using a novel technology provided by Firefly BioWorks (Boston, MA). The technology uses a unique post-hybridization ligation-based scheme to fluorescently label bound miRNA targets. Because RNA extraction is not needed with this technology, we were able to detect the miRNA array in a small volume of samples (300 μl) without the risk of losing RNA.

RNA extraction

Tissue and cell RNA extraction. Heart, spleen, or macrophages were disrupted and placed in TRIzol reagent. RNA was extracted according to the manufacturer's protocol. RNA in diethylpyrocarbonate-treated water was quantified and stored at −80°C for future experiments.

Plasma RNA extraction. Plasma was prepared from EDTA-anticoagulated blood. Two hundred microliters of plasma was mixed with 50 μl diethylpyrocarbonate-treated water and 750 μl TRIzol LS. *Caenorhabditis elegans* miR-39 was added as the spike-in control. Plasma RNA was extracted following the manufacturer's protocol, quantified using a Quant-iT RNA Assay Kit, and stored at −80°C for future experiments.

Cell treatments

Rat neonatal cardiomyocytes or bone marrow–derived macrophages were incubated in serum-free culture medium containing 0.05% BSA for 1 h prior to treatment with splenic RNA (10 μg/ml), miRNA mimics (50 nM), poly(I:C) (10 μg/ml), R837 (1 μg/ml), CL075 (1 μg/ml), or Pam3Cys (1 μg/ml) for the indicated time period. The miRNA mimic sequences are listed in Table I. Media or cells were collected for analysis. RNA, miRNA mimics, and poly(I:C) were complexed with the transfection agent Lipofectamine 3000 and incubated for 5 min at room temperature prior to the treatment. For the nuclease treatment in Fig. 2E, 4 μg RNA was incubated with RNase (10 μg) and DNase (1 U) at room temperature for 30 min before being complexed with Lipofectamine 3000.

qRT-PCR

Gene expression in cells and tissues. Cell and tissue RNA was extracted with TRIzol reagent and reverse transcribed to cDNA by a reverse-transcription reaction. cDNA was quantified using quantitative PCR, as described previously (25). The PCR primer sequences for host cellular RNA (3) and bacterial RNA (27) are listed in Table II. Transcript expression was calculated using the comparative Ct method normalized to GAPDH ($2^{-\Delta\Delta Ct}$) and expressed as the fold change in the CLP or treatment group over the sham or control group.

miRNA expression in plasma. Plasma RNA was extracted with TRIzol LS, as described above. Reverse transcription was performed using an miScript II RT kit. miRNA expression was analyzed using a miScript SYBR Green PCR Kit, following the manufacturer's protocol. Relative miRNA expression was calculated using the comparative Ct method normalized to spike-in *C. elegans* miR-39 ($2^{-\Delta\Delta Ct}$) and was expressed as the fold change in the CLP group over the sham group.

In vivo RNase administration and efficacy test

In vivo RNase administration and activity were tested as described previously with modifications (15). In brief, bovine pancreatic RNase A was dialyzed and filtered through a 30-kDa cut-off filter column and stored at 4°C. To test RNase activity, 3 mg RNase or the same volume of normal saline was administered s.c. Blood was collected at 3, 6, and 9 h after the injection. The serum was prepared and filtered through a 30-kDa filter column to remove large proteins. Filtered serum was incubated with 3 μg purified kidney RNA at 37°C for 2 h, followed by SYTO RNASelect green fluorescence staining and RNA electrophoresis. To test the impact of RNase administration on cardiac cfB expression in sepsis, RNase or normal saline was administered as follows: RNase 0.5 mg, i.p., 1 h before surgery, 3 mg s.c. immediately following surgery, and 3 mg s.c. 12 h after surgery. At 24 h, the hearts were harvested and stored at −80°C for future experiments.

Isolation and culture of cardiomyocytes and macrophages

Rat neonatal cardiomyocytes and mouse bone marrow–derived macrophages were isolated and cultured as described previously (3).

Immunoblotting of cfB, MAPKs, and IκBα

Medium proteins were separated in 4–12% gradient SDS-PAGE under reducing conditions, transferred to a polyvinylidene difluoride membrane, and blotted with goat anti-human cfB Ab. cfB protein bands were visualized using Luminata Forte Western HRP substrate. For MAPK and IκBα detection, macrophages were washed with cold Dulbecco's PBS and lysed in NP-40 buffer containing various protease and phosphatase inhibitors following treatments. Protein was quantified using the Bradford method, and equal amounts of protein were subjected to SDS-PAGE and immunoblotting.

Complement AP activity assay

AP activity was assayed as described previously (28), with modifications. AP activation was achieved in medium containing 11 μg/ml CVF (a functional C3b analog), cfB-deficient serum containing factor D, and 5 mM $MgCl_2$. In the presence of Mg^{2+}, CVF binds to cfB; it is cleaved by

Downloaded from http://journals.aai.org/jimmunol/article-pdf/196/6/2788/1417822/1502106.pdf by guest on 06 March 2025

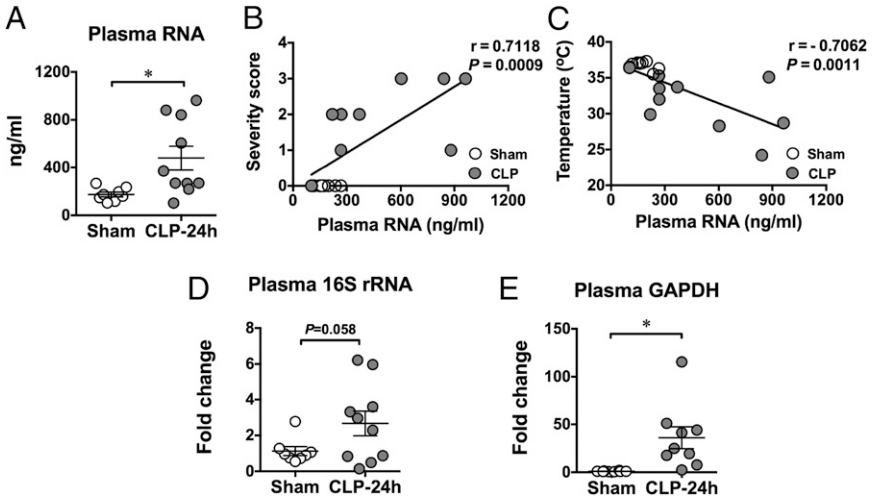

FIGURE 1. Polymicrobial sepsis leads to host and bacterial RNA release into the blood circulation. Twenty-four hours after sham or CLP surgery, mice were euthanized, and blood was collected via the inferior vena cava. RNA was extracted from plasma and quantified as described in *Materials and Methods*. (**A**) Plasma total RNA concentrations in sham and CLP mice ($n = 8$ in sham group, $n = 10$ in CLP group). Association of plasma RNA concentration and sepsis severity score (**B**) or core temperature (**C**). Sepsis severity score was monitored as detailed in *Materials and Methods*. Rectal temperature was recorded as the core temperature. $n = 18$ pair samples. (**D**) Bacterial 16S rRNA in the plasma, as measured by qRT-PCR. (**E**) Host GAPDH mRNA in the plasma, as measured by qRT-PCR ($n = 8$ in sham group, $n = 10$ in CLP group). $^{*}p < 0.05$.

factor D into Ba, which is released, and Bb, which remains bound to CVF. The CVF.Bb complex is a C3 convertase. The mixture was incubated in a 37°C water bath for 1 h. The assay solutions were mixed with SDS sample buffer and subjected to SDS-PAGE. Total cfB or Ba fragments were immunoblotted with a specific anti-cfB Ab.

In vivo administration of RNA and miRNA mimics

In vivo RNA and miRNA mimics administration was performed as previously described (18). In brief, after the fur was removed and the abdominal skin was disinfected, mice were injected i.p., using a 31-gauge needle insulin syringe, with Lipofectamine or Lipofectamine-complexed

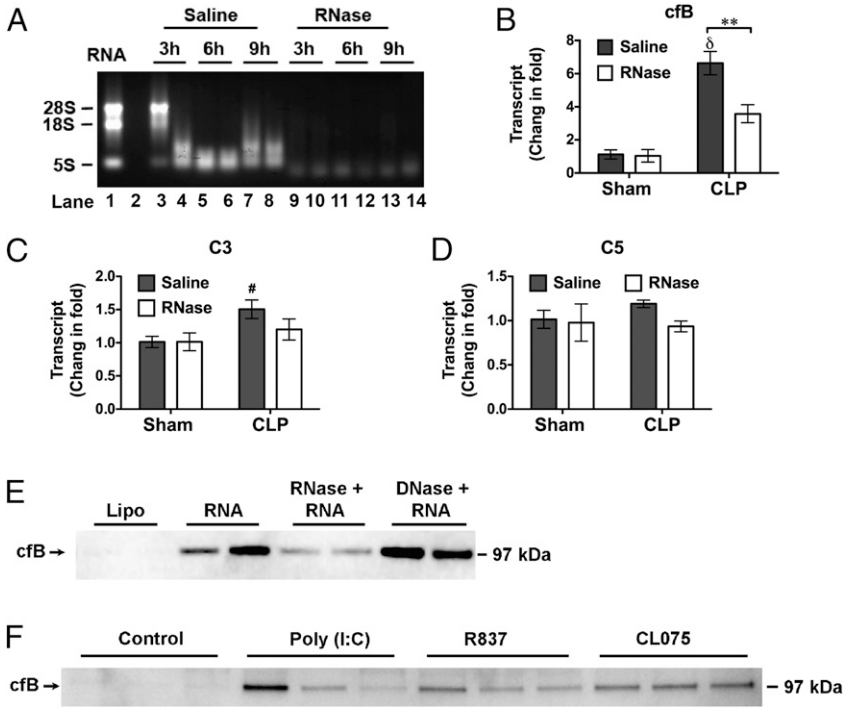

FIGURE 2. Role of RNA in cfB production in the heart and isolated cardiomyocytes. (**A**) RNA digestion by serum RNase: testing the efficacy of systemic administration of RNase. As detailed in *Materials and Methods*, sera were prepared from mice injected with saline or RNase A and incubated with 3 μg of purified RNA at 37°C for 2 h. *Lane 1*, Untreated RNA; *lanes 3–8*, RNA treated with serum from the mice injected with saline; *lanes 9–14*, RNA treated with serum from the mice injected with RNase A. Effect of systemic RNase administration on cardiac gene expression of cfB (**B**), C3 (**C**), and C5 (**D**). RNase was administered before and 12 h after sham or CLP surgery. cfB/C3/C5 gene expression was detected in the heart 24 h after surgery using qRT-PCR ($n = 4$/group). (**E**) Effect of RNase on RNA-induced cfB protein production. Cultured rat neonatal cardiomyocytes were treated with Lipofectamine alone (Lipo) or with cardiac RNA (10 μg/ml) for 24 h. As indicated, in some treatment groups, RNA was treated with RNase or DNase before being applied to cardiomyocyte cultures. Medium cfB was detected by Western blot, as described in *Materials and Methods*. (**F**) Effect of TLR ligands on cfB protein production in rat neonatal cardiomyocytes. Cardiomyocytes were treated with poly(I:C) (10 μg/ml), R837 (1 μg/ml), or CL075 (1 μg/ml) for 24 h. Medium cfB was detected with Western blot. $^{\#}p < 0.05$, $^{\delta}p < 0.001$ versus Sham-Saline, $^{**}p < 0.01$.

Downloaded from http://journals.aai.org/jimmunol/article-pdf/196/6/2788/1417822/1502106.pdf by guest on 06 March 2025

RNA (50 μg/mouse) or with Lipofectamine-complexed miR-146a (20 μg/mouse) or miR-146a mutant. The injection site was immediately covered with an adhesive 3M Tegaderm film to prevent any potential contamination and infection. Twenty hours later, 2 ml saline was injected into the peritoneal space and mixed thoroughly. Peritoneal lavage fluid was collected and centrifuged. The cell-free supernatant was stored at −80°C for further cfB protein analysis.

Statistical analysis

Statistical analysis was performed using GraphPad Prism 6 software (GraphPad, La Jolla, CA). The distributions of the continuous variables were expressed as mean ± SE. Two-way ANOVA with Bonferroni adjusted p value for post hoc analysis was applied to test the differences in cardiac cfB expression between the saline and RNase groups (Fig. 2B), cfB expression in macrophages among the WT, TLR7$^{-/-}$, and TLR3$^{-/-}$ groups (Figs. 3B, 5E), MAPKs/IκBα expression between the WT and TLR7$^{-/-}$ groups (Fig. 7B–E), the role of MAPK inhibitors on cfB expression (Fig. 7), and lavage fluid cfB protein expression among the WT, MyD88$^{-/-}$, and TLR7$^{-/-}$ groups (Fig. 9). Pearson correlation analysis was used to assess the relationship between plasma RNA concentration and rectal temperature, sepsis severity, or splenic cfB mRNA level. The relationship between plasma miRNA-146a, miRNA-122, miRNA-145, or miRNA-210 level and splenic cfB mRNA was also analyzed by Pearson correlation. The Student t test was used for statistical analysis between groups for all other data. The null hypothesis was rejected for $p < 0.05$ with the two-tailed test.

Results

Polymicrobial infection leads to an increase in circulating RNA

To determine whether cellular RNA was released into the circulation during bacterial infection, we created a CLP model of polymicrobial infection and tested the circulating RNA in sham and CLP mice. As shown in Fig. 1A, although there was a large variation among different infected mice, the mean RNA concentration in the plasma of CLP mice was significantly higher than that of sham mice (478.1 ± 100 versus 174.6 ± 20 ng/ml). Interestingly, the amount of circulating RNA correlated with the sepsis severity, as well as with body temperature of mice, including the sham and CLP groups (Fig. 1B, 1C). Mice with more severe sepsis and lower body core temperature tended to have higher circulating RNA levels. Moreover, we found that a significant amount of cell-free 16S rRNA, which is common to many species of bacteria, increased in the plasma of septic mice compared with the sham-operated mice (Fig. 1D). Similarly, the circulatory cell-free mRNA of GAPDH, which is stably and constitutively expressed at high levels in most tissues and cells, was also significantly increased in septic mice (Fig. 1E). These data suggest that, during polymicrobial infection, host cells and invading bacteria release their cellular RNA into the host circulation and that the circulating RNA level is associated with overall sepsis severity.

Eliminating extracellular RNA reduces cardiac cfB gene expression in septic mice

Our previous study established an important role for cfB and complement AP activation in septic cardiac dysfunction and mortality (3). In that study, we showed that cardiac cfB is markedly and specifically upregulated in response to polymicrobial infection. Lack of systemic cfB improves cardiac function, as well as survival of septic mice. To determine whether extracellular RNA contributes to cardiac cfB upregulation during bacterial sepsis, we treated mice with RNase A before and after CLP, with the aim of eliminating extracellular RNA. To determine the efficacy of RNase A administration, we tested serum RNase activity. As shown in Fig. 2A, when sera were incubated with purified cellular RNA, those derived from saline-injected mice possessed endogenous RNase activity, resulting in partial degradation of 28S/18S rRNA and, consequently, an increase in RNA of small m.w. around 5S (Fig. 2A, *lanes 3–8*). In comparison, systemic administration of exogenous RNase led to higher serum RNase activity between 3 and 9 h after injection, as

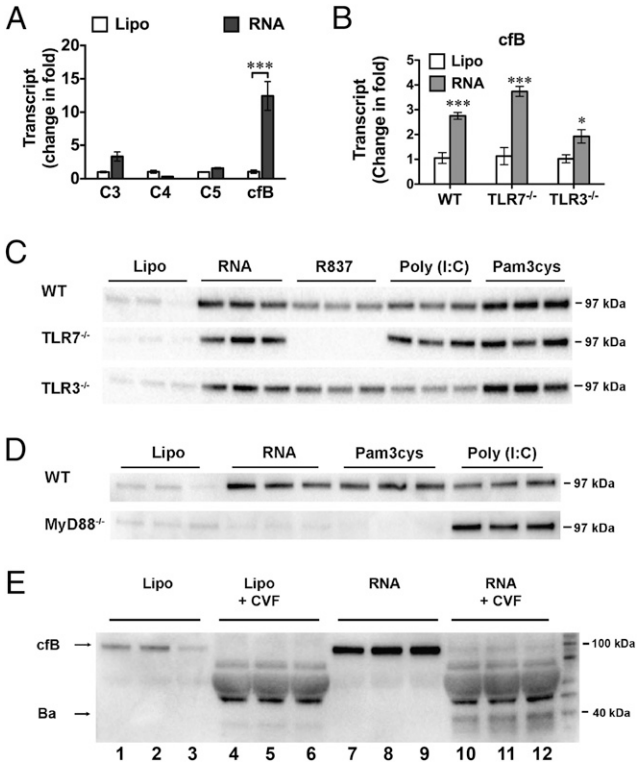

FIGURE 3. Splenic RNA-induced cfB production was mediated via MyD88 signaling in macrophages. (**A**) Complement gene expression in macrophages treated with splenic RNA. Mouse macrophages were treated with Lipofectamine (Lipo) alone or splenic RNA (10 μg/ml) complexed with Lipofectamine. Six hours later, C3, C4, C5, and cfB mRNA was analyzed by qRT-PCR (n = 3/group). The experiments were repeated three times. ***$p < 0.001$. (**B**) cfB gene expression in macrophages isolated from WT, TLR7$^{-/-}$, or TLR3$^{-/-}$ mice. Cells were treated with Lipofectamine (Lipo) alone or RNA (10 μg/ml) for 6 h (n = 3/group). *$p < 0.05$, ***$p <$ 0.001 versus the corresponding Lipo control. (**C**) Splenic RNA- and TLR ligand–induced cfB protein production in WT, TLR7$^{-/-}$, and TLR3$^{-/-}$ macrophages. Macrophages were treated with Lipofectamine, RNA (10 μg/ml), R837 (0.25 μg/ml), poly(I:C) (10 μg/ml), or Pam3Cys (1 μg/ml). Twenty-four hours later, medium cfB was analyzed. The experiment was repeated three times. (**D**) Impact of MyD88 on RNA- and TLR ligand–induced cfB production in the medium. The experiment was repeated twice. (**E**) AP activity assay. Macrophages were incubated in serum-free (complement-free) medium and treated with Lipofectamine (*lanes 1–6*) or 10 μg/ml RNA (*lanes 7–12*) for 24 h, as indicated. At the end of treatment, media were collected and incubated in the presence of 2.5% cfB$^{-/-}$ mouse serum, 11 μg/ml of CVF, and 5 mM of $MgCl_2$ at 37°C for 1 h and analyzed for cfB and Ba fragment by Western blot. The experiment was repeated twice.

demonstrated by almost complete digestion of cellular RNA, including 28S/18S rRNA and 5S small RNA (Fig. 2A, *lanes 9–14*). As shown in Fig. 2B and 2C, 24 h after CLP, there was a significant increase in cfB and a slight increase in C3 gene expression (fold change: cfB, 6.6 ± 0.7; C3, 1.5 ± 0.1), but not that of C5 (Fig. 2D), in the heart compared with the sham control. Importantly, there was a 46% reduction in cardiac cfB gene expression in septic mice treated with RNase before and after CLP compared with septic mice treated with saline alone (Fig. 2B). These data suggest that circulating RNA may contribute, in part, to cardiac cfB production during polymicrobial infection.

RNA and TLR ligands induce cfB production in cardiomyocytes

To determine the effect of cellular RNA on cardiac cfB production, we isolated rat neonatal cardiomyocytes and treated the cultured

Downloaded from http://journals.aai.org/jimmunol/article-pdf/196/6/2788/1417822/1502106.pdf by guest on 06 March 2025

cells with RNA that was isolated from mouse heart and complexed with Lipofectamine. As shown in Fig. 2E, 24 h after RNA treatment, there was a significant amount of cfB detected in the culture media, whereas there was minimal cfB detected in Lipofectamine-treated cells. The effect of the cardiac RNA was nearly completely abolished by pretreatment with RNase but not DNase. Moreover, media collected from cardiomyocyte cultures treated with TLR3 ligand [poly(I:C)], TLR7 ligand (R837), or TLR7/8 ligand (CL075) displayed elevated cfB levels compared with the Lipofectamine control (Fig. 2F).

Splenic RNA induces cfB production via MyD88 signaling

We next tested the effect of splenic RNA on complement gene expression in bone marrow–derived macrophages. As shown in Fig. 3A, consistent with what we found in cardiomyocytes, RNA induced a marked cfB gene expression, whereas it had a minimal effect on C3, C4, or C5 gene expression. A loss-of-function study indicated that neither TLR7 nor TLR3 gene deletion had a significant impact on RNA-induced cfB expression (Fig. 3B). This was confirmed by Western blot. Neither TLR7 nor TLR3 deficiency had any effect on the RNA-induced cfB protein production (Fig. 3C). Similar to cfB protein production in cardiomyocytes, R837 (TLR7 agonist) or poly(I:C) (TLR3 agonist) induced a significant increase in cfB protein production, and their effect was completely or nearly completely blocked in the cells lacking TLR7 or TLR3, respectively (Fig. 3C). The decrease in cfB in these TLR-deficient macrophages was not due to poor cell condition, as they had a normal response to Pam3Cys, a TLR2 ligand, compared with WT macrophages. In contrast, MyD88, an adaptor for all TLRs, with the exception of TLR3, completely blocked RNA- and TLR2-induced cfB production, but it had no impact on TLR3-mediated cfB protein production (Fig. 3D). Finally, to determine the biological activity of the de novo–synthesized cfB in macrophages treated with splenic RNA, we tested the ability of medium cfB to promote AP activity. As illustrated in Fig. 3E, compared with Lipofectamine (*lanes 1–3*), splenic RNA induced a marked increase in the cfB level in serum-free medium (*lanes 7–9*). In the presence of CVF (a functional C3b analog), there was increased AP activity, as demonstrated by increased cfB cleavage and consequent Ba generation (*lanes 10–12*). In contrast, treatment with CVF alone, without the newly synthesized medium cfB, only induced a minimal level of AP activity (*lanes 4–6*).

Plasma miRNA array in septic mice

To identify host miRNA released into the circulation during polymicrobial infection, we subjected mice to sham or CLP surgery. Twenty-four hours later, we collected the plasma from both groups of mice and tested them for miRNA expression using an miRNA array (Fig. 4A). The complete miRNA array data (accession number GSE74952) can be accessed at http://www.ncbi.nlm.nih.gov/geo/query/acc.cgi?acc=GSE74952. Among the 68 miRNAs reportedly related to immunologic functions, 6 miRNAs exhibited a >2-fold increase in the CLP mice compared with the sham control mice (CLP/sham ratio > 2), with fluorescence counts > 100 (Fig. 4B): miR-145-5p, miR-122-5p, miR-192-5p, miR-146a-5p, miR-34a-5p, and miR-210-3p. Fig. 4C illustrates the mean fluorescent intensity of these six miRNAs in both groups, as measured by the miRNA array. The differences in the fluorescent intensities of these six miRNAs between the sham and CLP groups were statistically significant (Fig. 4C). To validate these miRNA array results, we tested these six miRNAs using qRT-PCR in the plasma collected from a separate set of animals that underwent sham or CLP procedures. As shown in Fig. 4D, of the six miRNAs tested, four were confirmed to have a significant increase in septic mice compared with sham mice: miR-145-5p, miR-122-5p, miR-146a-5p, and miR-210-3p. To determine whether these miRNAs were capable of inducing cfB production, we treated macrophages with the miRNA mimics (Table I) complexed with Lipofectamine or Lipofectamine alone for 24 h. As shown in Fig. 5A, miR-146a, miR-34a, miR-122, and miR-145, all at 50 nM, induced a marked increase in cfB protein production in macrophages. In contrast, miR-192 and miR-210, at the same concentration, failed to induce cfB production. In the case of miR-146a, the cfB-inducing effect was sequence specific, because its U→A mutant failed to induce cfB production at the gene and protein

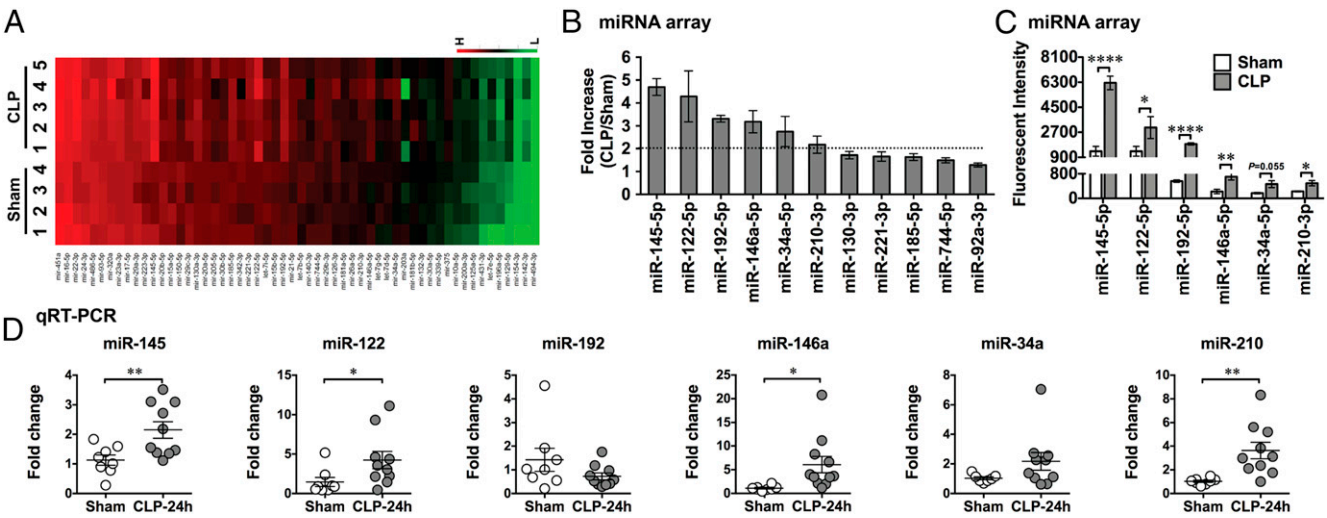

FIGURE 4. Plasma miRNA profiling in septic mice. (**A**) Heat map of miRNA array. Mice were subjected to sham surgery ($n = 4$) or CLP ($n = 5$). At 24 h, plasma was collected, and miRNAs were analyzed using a firefly miRNA array (Firefly BioWorks). The fluorescence intensity of 56 miRNAs was expressed from low (green) to high (red). (**B**) Fold change in the plasma miRNAs in CLP compared with Sham mice (CLP/Sham), as measured by miRNA array. (**C**) Mean fluorescent intensity of plasma miRNAs, as measured by miRNA array, in Sham and CLP mice. Six miRNAs (miR-145, miR-122, miR-192, miR-146a, miR-34a, miR-210) were significantly increased >2-fold in the septic mice compared with the sham control ($n = 4$ in sham group, $n = 5$ in CLP group). (**D**) qRT-PCR validation of miRNAs. The six target miRNAs were tested using qRT-PCR in a separate set of plasma ($n = 8$ in sham group, $n = 10$ in CLP group). $^*p < 0.05$, $^{**}p < 0.01$, $^{****}p < 0.001$.

Downloaded from http://journals.aai.org/jimmunol/article-pdf/196/6/2788/1417822/1502106.pdf by guest on 06 March 2025

Table I. Sequences of miRNA mimics

miRNA	Sequence (5′–3′)
mmu-miR-146a-5p	UGAGAACUGAAUUCCAUGGGUU
mmu-miR-145-5p	GUCCAGUUUUCCCAGGAAUCCCU
mmu-miR-122-5p	UGGAGUGUGACAAUGGUGUUUG
mmu-miR-34a-5p	UGGCAGUGUCUUAGCUGGUUGU
mmu-miR-210-3p	CUGUGCGUGUGACAGCGGCUGA
mmu-miR-192-5p	CUGACCUAUGAAUUGACAGCC

levels (Fig. 5B, 5C). The effect of miR-146a also appeared to be specific for cfB, because it only induced and led to a mild increase in C3 and none in C4 or C5 gene expression in macrophages (Fig. 5B, Table II). Moreover, similar to the splenic RNA–induced cfB response, miR-146a–induced cfB synthesis in macrophages promoted AP activation. As illustrated in Fig. 5D, de novo–synthesized cfB was released from macrophages stimulated by miR-146a (*lanes 7–12*) and, in the presence of the functional C3b analog CVF and cfB$^{-/-}$ serum containing factor D and Mg^{2+}, led to AP activation, as evidenced by increased cfB cleavage and Ba formation (*lanes 10–12*). In contrast, miR-146a mutant failed to induce cfB production or AP activation (*lanes 1–6*).

miR-146a induces cfB production via TLR7-MyD88 signaling in macrophages

We tested miR-146a for its signaling pathway in mediating cfB production. As shown in Fig. 5E and 5F, treatment with miR-146a led to a marked increase in cfB gene and protein expression. The effect was completely blocked in TLR7$^{-/-}$ macrophages, but it was not affected in TLR3$^{-/-}$ macrophages. Moreover, R837 and poly(I:C) induced a robust cfB production, and their effects were specifically blocked in TLR7$^{-/-}$ and TLR3$^{-/-}$ macrophages, respectively. In contrast, Pam3Cys, a TLR2 ligand, maintained its ability to induce cfB synthesis in WT and TLR3- and TLR7-deficient macrophages. Finally, the effect of miR-146a seemed to be completely dependent on MyD88 signaling, because it failed to induce cfB synthesis in MyD88$^{-/-}$ macrophages (Fig. 5G). As anticipated, Pam3Cys (TLR2), but not poly(I:C) (TLR3), induced cfB production via a MyD88-dependent mechanism.

miR-146a activates MAPKs and NF-κB via TLR7 signaling

To investigate the downstream signaling of miR-146a, we examined the intracellular MAPK and NF-κB pathways. WT macrophages were stimulated with 50 nM miR-146a for a period of 60, 90, or 120 min. Immunoblotting of the cell lysates revealed a strong phosphorylation of p38, JNK, and ERK1/2, with the peak

Downloaded from http://journals.aai.org/jimmunol/article-pdf/196/6/2788/1417822/1502106.pdf by guest on 06 March 2025

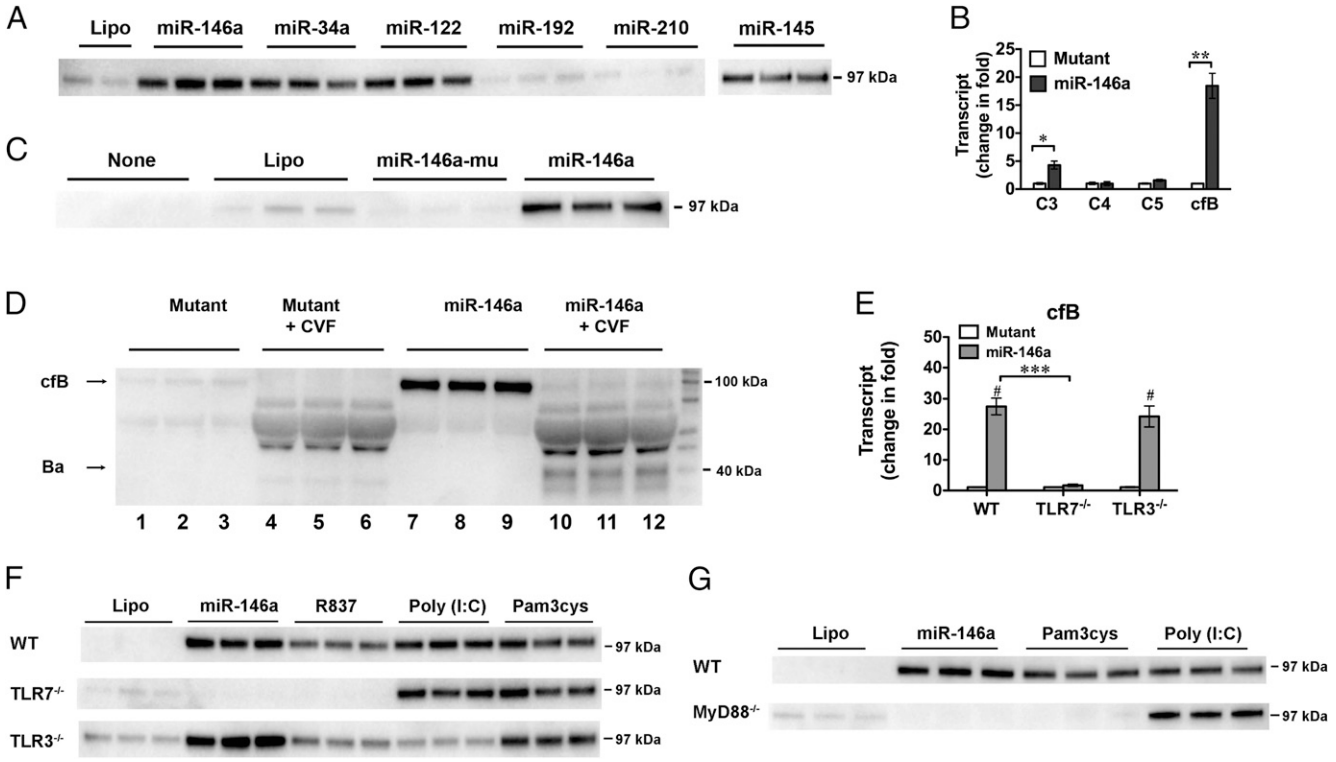

FIGURE 5. miRNA-induced cfB production occurs via TLR7-MyD88 signaling in the macrophage. (**A**) miRNA mimics induce cfB production. Macrophages were treated with 50 nM of miRNAs for 18 h, and media were analyzed for cfB expression. (**B**) Effect of miR-146a on complement gene expression in macrophages. miR-146a mimic or miR-146a mutant (50 nM) was incubated with WT macrophages. Six hours later, C3, C4, C5, and cfB mRNAs were measured using qRT-PCR (n = 3/group). The experiment was repeated twice. (**C**) Effect of miR-146a and its U→A mutant on cfB protein production in the medium. (**D**) AP activity assay. Macrophages were incubated in serum-free (complement-free) medium and treated with 50 nM of miR-146a mutant (*lanes 1–6*) or miR-146a (*lanes 7–12*) for 24 h. At the end of treatment, media were collected and incubated in the absence (*lanes 1–3* and *7–9*) or presence (*lanes 4–6* and *10–12*) of 2.5% cfB$^{-/-}$ mouse serum, 11 μg/ml CVF, and 5 mM $MgCl_2$ at 37°C for 1 h and analyzed for cfB and Ba fragment by Western blot. The experiment was repeated twice. (**E**) Impact of TLR7 and TLR3 deletion on miR-146a–induced cfB gene expression. WT, TLR3$^{-/-}$, and TLR7$^{-/-}$ macrophages were treated with miR-146a (50 nM) or its mutant for 6 h. cfB mRNA was quantified by qRT-PCR (n = 3/group). The experiment was repeated twice. (**F**) Impact of TLR7 and TLR3 deletion on miR-146a–induced cfB protein production. Macrophages from WT, TLR3$^{-/-}$, and TLR7$^{-/-}$ mice were treated with Lipofectamine, miR-146a (50 nM), R837 (0.25 μg/ml), poly(I:C) (10 μg/ml), or Pam3Cys (1 μg/ml) for 18 h. Media were collected for cfB analysis. The experiment was repeated twice. (**G**) Effect of MyD88 deletion on miR-146a–induced cfB protein production. Cells were treated with Lipofectamine, miR-146a, Pam3Cys, or poly(I:C) for 18 h, and the culture media were tested for cfB expression. The experiment was repeated twice. $^{*}p < 0.05$, $^{**}p < 0.01$, $^{***}p < 0.001$, $^{\#}p < 0.001$ versus the corresponding mutant control. Lipo, Lipofectamine.

Table II. Primer sequences for qRT-PCR

Gene	Primer Sequence
Mouse GAPDH	Forward 5′-AACTTTGGCATTGTGGAAGG-3′
	Reverse 5′-GGATGCAGGGATGATGTTCT-3′
Mouse C3	Forward 5′-GGCAAGACAGTCGTCATCCT -3′
	Reverse 5′-CCAAGACAAAGGCAAGATGC -3′
Mouse C5	Forward 5′-TACCACAGAACCCAGGAGGA -3′
	Reverse 5′-GCCATCCGCAGGTATGTTAG -3′
Mouse cfB	Forward 5′-GAAACCCTGTCACTGTCATTC -3′
	Reverse 5′-CCCCAAACACATACACATCC-3′
Bacterial 16S rRNA (27)	Forward 5′-ATTAGATACCCTGGTAGTCCACGCC-3′
	Reverse 5′-CGTCATCCCCACCTTCCTCC-3′

effect seen between 90 and 120 min (Fig. 6A). R837, a TLR7 ligand, but not the miR-146a mutant induced a similar effect as miR-146a (Fig. 6B–D). MAPK activation appeared to be mediated via TLR7, because TLR7$^{-/-}$ macrophages failed to respond to miR-146a or R837 (Fig. 6B–D). Activation of NF-κB involves the phosphorylation and proteolysis of the IκB-α protein and, subsequently, nuclear translocation of the NF-κB factors. As shown in Fig. 6E, stimulation of macrophages with miR-146a (not its mutant) led to the degradation of IκB-α, suggesting an activation of NF-κB signaling in the miR-146a–treated cells. In contrast, the IκB-α protein level was maintained at the baseline level in TLR7$^{-/-}$ macrophages, despite miR-146a treatment.

Inhibition of JNK/p38 and NF-κB signaling attenuates miR-146a–induced cfB production

To determine whether MAPKs and NF-κB activation are involved in cfB de novo synthesis in response to miR-146a treatment, we treated cultured macrophages with specific inhibitors of p38, JNK, ERK1/2, or NF-κB. As shown in Fig. 7A, miR-146a induced a robust response in cfB gene expression compared with its U→A mutant. Pretreatment of macrophages with the inhibitor of p38 or JNK markedly reduced the miR-146a–induced cfB gene expression. Bay 11-7082, an inhibitor of IκB-α kinase, completely blocked the cfB gene expression induced by miR-146a. In contrast, blocking of ERK signaling by MEK1/2 inhibitor PD98059 or U0126 significantly enhanced the miR-146a–mediated cfB gene expression (Fig. 7B, 7C).

Splenic cfB expression is correlated with plasma RNA and miRNAs during polymicrobial infection

As shown in Fig. 8A, 24 h after CLP, there was a significant increase in cfB gene expression in the spleen compared with sham-operated mice. To determine the relationship between splenic cfB expression and plasma RNA/miRNA levels, we plotted the two

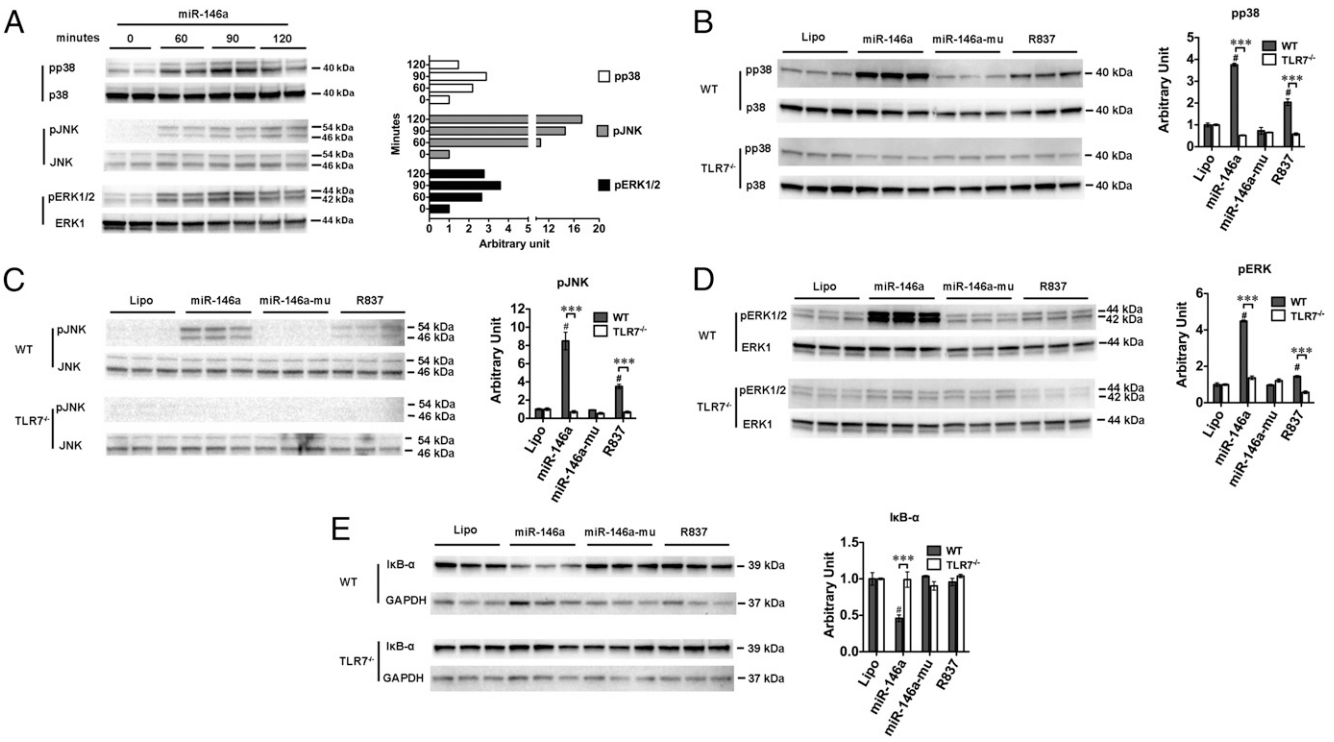

FIGURE 6. miR-146a activates MAPK and NF-κB signaling via TLR7. (**A**) Immunoblotting of p38, JNK, and ERK1/2. Macrophages were treated with 50 nM of miR-146a. At time 0, 60, 90, and 120 min, cells were lysed and tested for phosphorylated and total p38, JNK, and ERK1/2. The difference was expressed as the ratio to time 0, as quantified by Image J. TLR7 deletion completely blocked miR-146a– or R837-induced phosphorylation of p38 (**B**), JNK (**C**), and ERK1/2 (**D**). WT and TLR7$^{-/-}$ macrophages were treated with miR-146a (50 nM) or R837 (0.25 μg/ml) for 90 min. Cell lysates were extracted and analyzed for phosphorylation of p38, JNK, and ERK1/2. Total MAPK expression served as the internal control (n = 3/group). The difference was expressed as the ratio to Lipofectamine control (Lipo) in each strain, as quantified by Image J. (**E**) TLR7 deletion blocked miR-146a–induced IκB-α degradation. GAPDH served as the protein-loading control (n = 3/group). The difference was expressed as the ratio to Lipofectamine control (Lipo) in each strain, as quantified by ImageJ. $^{\#}p < 0.001$ versus Lipofectamine control (Lipo), $^{***}p < 0.001$, WT versus TLR7$^{-/-}$ group.

Downloaded from http://journals.aai.org/jimmunol/article-pdf/196/6/2788/1417822/1502106.pdf by guest on 06 March 2025

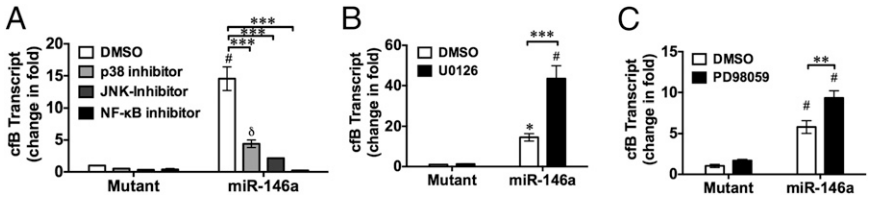

FIGURE 7. Inhibition of JNK, p38, and NF-κB attenuates miR-146a–induced cfB gene expression. WT macrophages were incubated with (**A**) p38 inhibitor (SB203580, 20 μM), JNK inhibitor II (SP600125, 20 μM), NF-κB signaling inhibitor (Bay 11-7082, 10 μM), or (**B** and **C**) ERK inhibitors (U0126, 10 μM; PD 98095, 20 μM) for 1 h prior to treatment with miR-146a (50 nM) or its U→A mutant. cfB mRNA level was quantified by qRT-PCR 6 h after treatment (n = 3/group). $^{*}p < 0.05$, $^{\delta}p < 0.01$, $^{\#}p < 0.001$ versus corresponding mutant control, $^{**}p < 0.01$, $^{***}p < 0.001$.

sets of data (splenic cfB versus plasma RNA or miRNAs) from the sham and CLP groups. As shown in Fig. 8B–F, splenic cfB expression was significantly correlated with the plasma RNA and miRNA (miR-145, miR-122, miR-146a, miR-210) levels. The r values ranged between +0.49 and +0.73.

RNA and miR-146a activate cfB production in vivo

To test whether in vivo administration of RNA or miRNA mimics was able to induce cfB production, we injected tissue RNA or miR-146a into the peritoneal cavity. Twenty hours later, the peritoneal lavage fluid was collected and tested for cfB protein level. As shown in Fig. 9, i.p. injection of splenic RNA or miR-146a in WT mice induced an increase in cfB expression in the peritoneal cavity compared with the controls (Lipofectamine and miR-146 mutant, respectively). Somewhat similar to cfB production in RNA-treated macrophages in vitro, the RNA-induced cfB production in vivo was dependent, in part, on MyD88, because $MyD88^{-/-}$ mice had significantly lower peritoneal cfB expression compared with WT mice (Fig. 9A). In contrast, systemic deletion of TLR7 completely prevented the miR-146a–induced cfB production in vivo (Fig. 9B).

Discussion

We previously documented a critical role for cfB and complement AP activation in an animal model of polymicrobial sepsis (3). Peritoneal bacterial infection induces marked systemic and local tissue expression of cfB and AP activation. Systemic cfB deficiency results in improved survival and organ functions in animals subjected to severe sepsis. However, the cellular and molecular mechanisms responsible for cfB upregulation and AP activation in the context of bacterial sepsis remain largely unexplored. In the current study, we tested the hypothesis that severe sepsis leads to release of bacterial and host cellular RNA into the circulation and that cellular RNA, such as miRNAs, is capable of inducing cfB production and AP activation. We found a significant increase in bacterial and host RNA in the plasma of septic animals. The plasma RNA concentration was closely associated with sepsis severity. Also, the plasma RNA and selective miRNA levels correlated with splenic cfB expression during polymicrobial sepsis. miRNA array identified, and qRT-PCR confirmed, a multifold increase in the plasma level of four host miRNAs (miR-146a, miR-145, miR-122, and miR-210) in septic mice. Moreover, treatment of cardiomyocytes and macrophages with splenic RNAs or the synthetic miRNA mimics (miR-146a, miR-145, miR-122, miR-34a) induced a robust cfB production and AP activation. In vivo, i.p. injection of RNA or miR-146a led to a significant increase in peritoneal cfB expression. Loss-of-function experiments demonstrated that signaling via MyD88 was important for RNA-induced cfB production in macrophages and in intact animals, as well as that TLR7 signaling was critical for the miR-146a–induced cfB production in vitro and in vivo. Finally, we showed that miR-146a mimic activated intracellular MAPKs and NF-κB signaling via TLR7 signaling and that inhibition of p38, JNK, and NF-κB signaling, but not ERK, led to a significant reduction in miRNA-146a–mediated cfB gene expression in macrophages.

Cell apoptosis and necrosis occur in severe sepsis and are associated with the mortality of septic animals (29, 30). The injured cells release danger-associated molecules, such as nucleic acids, HMGB1, heat shock proteins, and mitochondrial components, which trigger innate immune responses like cytokine production, immune cell activation and recruitment, and free radical species production (31). In an effort to search for an endogenous mediator (s) for cfB production during polymicrobial sepsis, we hypothesized that cellular RNA released as a result of tissue injury during sepsis is capable of inducing cfB de novo synthesis. Our observations that systemic RNase administration attenuates myocardial cfB gene expression and that plasma RNA concentration is correlated with splenic cfB expression during bacterial infection are

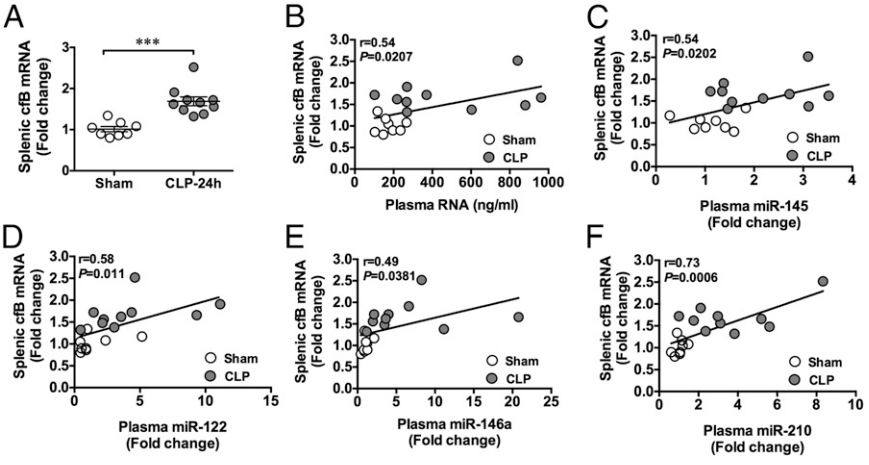

FIGURE 8. Splenic cfB gene expression correlates with plasma RNA and miRNAs during polymicrobial sepsis. Mice were subjected to sham surgery or CLP. Twenty hours later, the plasma and spleens were collected and extracted for total RNA. The plasma RNA concentrations were measured and analyzed for miRNAs, as indicated, using qRT-PCR. Splenic RNA was measured for cfB mRNA. (**A**) Splenic cfB mRNA expression (n = 8 in sham group, n = 10 in CLP group). (**B**) Association of plasma RNA concentrations and splenic cfB mRNA expression (n = 18 pair samples). Association of plasma miR-145 (**C**), miR-122 (**D**), miR-146a (**E**), and miR-210 (**F**) levels with splenic cfB mRNA expression (n = 18 pair samples). $^{***}p < 0.001$.

Downloaded from http://journals.aai.org/jimmunol/article-pdf/196/6/2788/1417822/1502106.pdf by guest on 06 March 2025

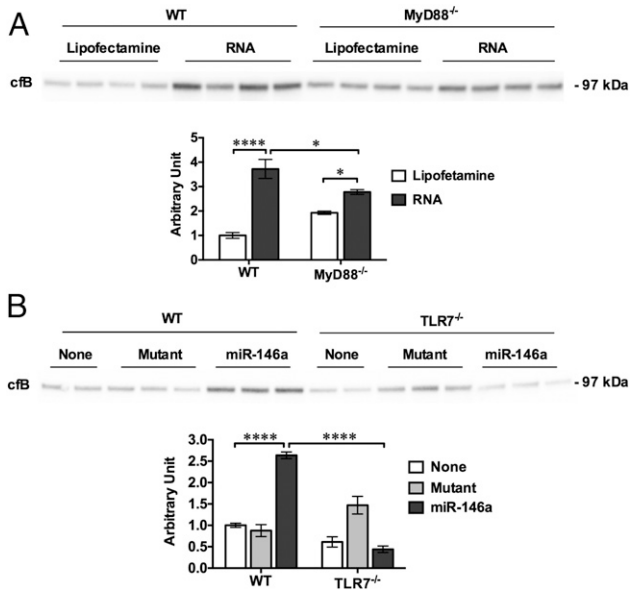

FIGURE 9. Cellular RNA and miR-146a mimics stimulate cfB production in vivo via TLR signaling. RNA (50 μg/mouse) or miR-146a (20 μg/mouse) complexed with Lipofectamine was injected i.p. into WT, MyD88$^{-/-}$, or TLR7$^{-/-}$ mice, with Lipofectamine or mutant as the respective control. Twenty hours later, peritoneal lavage fluid was harvested, and cfB protein expression was analyzed by Western blot. The cfB expression levels were quantitated by ImageJ software and expressed as the fold change over Lipofectamine control or no-injection group in WT mice. (**A**) cfB expression in peritoneal lavage fluid after RNA injection (n = 4/group). (**B**) cfB expression in peritoneal lavage fluid after miRNA-146a injection (n = 2–3/group). *$p < 0.05$, ****$p < 0.0001$. Mutant, miR-146a mutant.

consistent with the notion that extracellular RNA is responsible, in part, for cfB expression in the septic organs and provides us a clear rationale to test the ability of cellular RNA to activate cfB production. Indeed, our in vitro experiments demonstrate that tissue-derived RNA is capable of inducing a robust cfB production in, and release from, cardiomyocyte and macrophage cultures. This effect is clearly mediated by RNA because RNase, not DNase, near completely inhibits the RNA-induced cfB production. To assess the biological activity of the de novo–synthesized cfB, we tested AP activation in the media derived from the macrophage cultures treated with splenic RNA in the presence of CVF (a C3b analog) and cfB-deficient serum containing complement factor D and supplemented with Mg^{2+}. The increase in medium Ba fragments in the RNA-treated macrophage cultures demonstrates that RNA-induced cfB can bind to CVF and actively participates in the complement AP activation. Of note, although splenic RNA was used in most of the experiments in this study, the ability of cellular RNA to trigger cfB production does not appear to be organ or tissue specific, because cellular RNA isolated from mouse heart exhibits a similar effect. Moreover, the ability of cellular RNA to activate cfB production was further demonstrated in vivo following i.p. injection of cardiac RNA. Finally, in a separate study, we observed that cardiac cellular RNA from human, rat, and mouse, as well as extracellular RNA released from injured cardiomyocytes, exhibit the ability to induce various cytokine responses in cardiomyocytes and macrophages (18). Taken together, these data demonstrate that a significant amount of cellular RNA is released during bacterial sepsis and that host cellular RNA is capable of activating cfB production and promoting AP activation.

TLR3 and TLR7 are two important innate immune receptors that reportedly sense RNA of viral origin (32–34). TLR3 senses dsRNA and signals primarily through Trif, whereas TLR7 senses ssRNA and signals via MyD88 (35). The finding that several TLR ligands, including Pam3Cys, poly(I:C), R837, and CL075, induce cfB production in cardiomyocytes and macrophages suggests that activation of TLR2, TLR3, TLR7, and TLR8 is probably sufficient to initiate cfB synthesis. However, when we tested cfB production in macrophages of several knockout mice and compared it with that in WT mice, we found that TLR3 and TLR7 deficiency did not have any impact on the cellular RNA-induced complement synthesis. This was somewhat surprising because several previous studies suggested the role of TLR3 in sensing endogenous RNA. Karikó et al. (36) reported that in vitro–transcribed mRNA elicits cytokine production via a TLR3-dependent mechanism in human dendritic cells. A recent study by Bernard et al. (37) showed that RNA from UVB-irradiated keratinocytes induces cytokine production in normal human epidermal keratinocytes via TLR3. Moreover, in a stably transfected human HEK 293 cell line, in vitro–transcribed mRNA can induce cytokine production via a TLR7- and TLR8-dependent mechanism (38). Moreover, we show that cardiac RNA elicits cytokine production, in part, via TLR7-dependent signaling (18). Nevertheless, the current study found that MyD88 deficiency abolished the effect of RNA in vitro and partially in vivo, suggesting an important role for MyD88 signaling in mediating the cellular RNA–induced cfB response. Several possibilities may explain these data. TLR8, which, like TLR7, recognizes ssRNA, could mediate the effect of splenic RNA via MyD88-dependent signaling. In humans, TLR8, but not TLR7, is responsible for ssRNA-induced cytokine response. HEK 293 cells expressing human TLR8, but not TLR3 or TLR7, respond to viral RNA40 (39) or human mitochondrial RNA (38). However, although TLR7 and TLR8 are closely related phylogenetically, mouse TLR8 was thought to be nonfunctional (34). Alternatively, splenic RNA may signal through all three RNA sensors (i.e., TLRs 3/7/8) to induce the complement response, because ssRNA and dsRNA may exist in the spleen. Lacking one of them may prove insufficient to affect the final outcome (i.e., cfB production and AP activation) because of the shared and somewhat redundant signaling pathways among the three RNA sensors. Finally, it is also possible, although probably less likely, that different cell responses to RNA may depend on different RNA sensors and that RNA from different tissues (e.g., splenic versus cardiac RNA) may use different RNA sensors.

We used miRNA array to identify the different expression of plasma miRNAs between the sham and CLP mice. As validated by qRT-PCR, we identified four miRNAs (miR-146a, miR-145, miR-122, and miR-210) that were significantly elevated in the septic mice compared with the sham control. The miRNA array was limited and contained only 68 miRNAs. It is likely that the actual number of miRNAs being upregulated during polymicrobial sepsis is higher. An excellent study by Wu et al. (14) used a similar approach and identified that 10 of >1000 miRNAs tested were upregulated in the whole blood and serum following CLP. Interestingly, although it is well documented that TLR signaling (e.g., TLR2, TLR4, and TLR5) promotes miRNA biogenesis, and miRNAs regulate TLR signaling (40–42), this study found that systemic deficiency of TLR2, TLR4, or NF-κB had no significant impact on the serum miRNA upregulation induced by CLP (14).

Expanding the miRNA array assays, we tested the biological activities of the identified miRNAs. We found that miR-146a, miR-145, miR-122, and miR-34a induced a significant cfB production in macrophages. miR-146a is an immediate early-response gene induced by various microbial components and proinflammatory mediators. It reportedly inhibits TLR and cytokine signaling by

Downloaded from http://journals.aai.org/jimmunol/article-pdf/196/6/2788/1417822/1502106.pdf by guest on 06 March 2025

targeting IRAK-1 and TRAF-6 translation (40), and it is widely known for its role in the negative regulation of inflammation and endotoxin response (42–46). In contrast to these studies, the current study identified a novel role for miR-146a: promoting the innate immune complement response by stimulating cfB de novo synthesis and AP activation. Moreover, we found that the effect of miR-146a mimic was entirely dependent on TLR7 signaling, because TLR7 deficiency completely blocked the miR-146–induced cfB production in macrophages and in the peritoneum following i.p. injection.

Consistent with these findings, several previous studies demonstrated the role of extracellular miRNA as a signal molecule via TLR7. Fabbri et al. (47) reported that miR-21 and miR-29a secreted by tumor cells bind to TLR7 and activate the receptors in immune cells, leading to TLR-mediated NF-κB activation and secretion of prometastatic inflammatory cytokines. Another secreted extracellular miRNA, let-7, also reportedly activates TLR7 signaling and mediates pain (48) or causes neurodegeneration (49). These data suggest that miRNA, similar to ssRNA from virus (39), can be recognized by TLR7 and induce an inflammatory response. Of note, we could not identify any consensus pattern of oligonucleotide sequences among the miRNAs that induce cfB production. However, all four miRNAs that exhibit a strong ability to activate cfB synthesis are rich in U nucleotides (seven to nine Us), accounting for 30–40% of their entire sequences. This is inconsistent with the report by Heil et al. (39) that U-rich or U/G-rich oligonucleotides are essential for TLR7 recognition of ssRNA. Indeed, the U→A mutants of miR-146a abolished its ability to induce cfB synthesis in macrophages.

One of the major signaling families that participates in the intracellular transmission of extracellular signals is the MAPK. MAPKs are composed of serine/threonine kinases that phosphorylate and activate each other (50, 51). ERK1/2, p38, and JNK1/2 have been well studied in the context of innate immunity (52). Together with NF-κB signaling, these MAPKs participate in regulation of the cellular inflammatory response. The current finding that miRNA-146a, but not its U→A mutant, elicited phosphorylation of MAPKs and enhanced degradation of IκB-α, suggests that miR-146a signals through these MAPKs and activates NF-κB pathways. The data derived from WT and TLR7$^{-/-}$ macrophages demonstrate that miR-146a induces these intracellular events exclusively via TLR7 sensing. Importantly, using specific inhibitors, our data further demonstrate that miR-146a activates cfB production via a p38-, JNK-, and NF-κB–dependent mechanism. Interestingly, the ERK inhibitor enhanced the cfB-inducing effect of miR-146a, suggesting that ERK may negatively regulate cfB synthesis upon miR-146 stimulation.

In summary, the current study showed that polymicrobial sepsis induced a significant increase in the plasma RNA level, which encompassed bacterial and host cellular RNAs, including several miRNAs (e.g., miR-146a, miR-145, miR-122, and miR-210). Treatment with endogenous tissue RNA or the synthetic miRNA mimics, such as miR-146a, induces de novo cfB synthesis in, and release from, cultured cardiomyocytes and macrophages in vitro, as well as in the peritoneal space, when injected i.p. in vivo. Both RNA and miR-146a elicited cfB production via similar and specific innate immune and intracellular MAPK signaling mechanisms. Thus, our study identified a novel role for splenic/cardiac RNA and selective miRNAs in promoting complement AP via specific innate immune signaling.

Disclosures

The authors have no financial conflicts of interest.

References

1. Deutschman, C. S., and K. J. Tracey. 2014. Sepsis: current dogma and new perspectives. *Immunity* 40: 463–475.
2. Walport, M. J. 2001. Complement. First of two parts. *N. Engl. J. Med.* 344: 1058–1066.
3. Zou, L., Y. Feng, Y. Li, M. Zhang, C. Chen, J. Cai, Y. Gong, L. Wang, J. M. Thurman, X. Wu, et al. 2013. Complement factor B is the downstream effector of TLRs and plays an important role in a mouse model of severe sepsis. *J. Immunol.* 191: 5625–5635.
4. Mollnes, T. E., W. C. Song, and J. D. Lambris. 2002. Complement in inflammatory tissue damage and disease. *Trends Immunol.* 23: 61–64.
5. Niederbichler, A. D., L. M. Hoesel, M. V. Westfall, H. Gao, K. R. Ipaktchi, L. Sun, F. S. Zetoune, G. L. Su, S. Arbabi, J. V. Sarma, et al. 2006. An essential role for complement C5a in the pathogenesis of septic cardiac dysfunction. *J. Exp. Med.* 203: 53–61.
6. Zhang, X., Y. Kimura, C. Fang, L. Zhou, G. Sfyroera, J. D. Lambris, R. A. Wetsel, T. Miwa, and W. C. Song. 2007. Regulation of Toll-like receptor-mediated inflammatory response by complement in vivo. *Blood* 110: 228–236.
7. Harboe, M., and T. E. Mollnes. 2008. The alternative complement pathway revisited. *J. Cell. Mol. Med.* 12: 1074–1084.
8. Pratt, J. R., S. A. Basheer, and S. H. Sacks. 2002. Local synthesis of complement component C3 regulates acute renal transplant rejection. *Nat. Med.* 8: 582–587.
9. Farrar, C. A., W. Zhou, T. Lin, and S. H. Sacks. 2006. Local extravascular pool of C3 is a determinant of postischemic acute renal failure. *FASEB J.* 20: 217–226.
10. Daha, M. R., and C. van Kooten. 2000. Is there a role for locally produced complement in renal disease? *Nephrol. Dial. Transplant.* 15: 1506–1509.
11. Morgan, B. P., and P. Gasque. 1997. Extrahepatic complement biosynthesis: where, when and why? *Clin. Exp. Immunol.* 107: 1–7.
12. Kaczorowski, D. J., A. Afrazi, M. J. Scott, J. H. Kwak, R. Gill, R. D. Edmonds, Y. Liu, J. Fan, and T. R. Billiar. 2010. Pivotal advance: The pattern recognition receptor ligands lipopolysaccharide and polyinosine-polycytidylic acid stimulate factor B synthesis by the macrophage through distinct but overlapping mechanisms. *J. Leukoc. Biol.* 88: 609–618.
13. Bleiblo, F., P. Michael, D. Brabant, C. V. Ramana, T. Tai, M. Saleh, J. E. Parrillo, A. Kumar, and A. Kumar. 2012. The role of immunostimulatory nucleic acids in septic shock. *Int. J. Clin. Exp. Med.* 5: 1–23.
14. Wu, S. C., J. C. Yang, C. S. Rau, Y. C. Chen, T. H. Lu, M. W. Lin, S. L. Tzeng, Y. C. Wu, C. J. Wu, and C. H. Hsieh. 2013. Profiling circulating microRNA expression in experimental sepsis using cecal ligation and puncture. *PLoS One* 8: e77936.
15. Chen, C., Y. Feng, L. Zou, L. Wang, H. H. Chen, J. Y. Cai, J. M. Xu, D. E. Sosnovik, and W. Chao. 2014. Role of extracellular RNA and TLR3-Trif signaling in myocardial ischemia-reperfusion injury. *J. Am. Heart Assoc.* 3: e000683.
16. Cabrera-Fuentes, H. A., M. Ruiz-Meana, S. Simsekyilmaz, S. Kostin, J. Inserte, M. Saffarzadeh, S. P. Galuska, V. Vijayan, I. Barba, G. Barreto, et al. 2014. RNase1 prevents the damaging interplay between extracellular RNA and tumour necrosis factor-α in cardiac ischaemia/reperfusion injury. *Thromb. Haemost.* 112: 1110–1119.
17. Fischer, S., T. Grantzow, J. I. Pagel, M. Tschernatsch, M. Sperandio, K. T. Preissner, and E. Deindl. 2012. Extracellular RNA promotes leukocyte recruitment in the vascular system by mobilising proinflammatory cytokines. *Thromb. Haemost.* 108: 730–741.
18. Feng, Y., H. Chen, J. Cai, L. Zou, D. Yan, G. Xu, D. Li, and W. Chao. 2015. Cardiac RNA induces inflammatory responses in cardiomyocytes and immune cells via Toll-like receptor 7 signaling. *J. Biol. Chem.* 290: 26688–26698.
19. Small, E. M., R. J. Frost, and E. N. Olson. 2010. MicroRNAs add a new dimension to cardiovascular disease. *Circulation* 121: 1022–1032.
20. van Rooij, E. 2012. Introduction to the series on microRNAs in the cardiovascular system. *Circ. Res.* 110: 481–482.
21. Krol, J., I. Loedige, and W. Filipowicz. 2010. The widespread regulation of microRNA biogenesis, function and decay. *Nat. Rev. Genet.* 11: 597–610.
22. Creemers, E. E., A. J. Tijsen, and Y. M. Pinto. 2012. Circulating microRNAs: novel biomarkers and extracellular communicators in cardiovascular disease? *Circ. Res.* 110: 483–495.
23. Chen, X., H. Liang, J. Zhang, K. Zen, and C. Y. Zhang. 2012. Secreted microRNAs: a new form of intercellular communication. *Trends Cell Biol.* 22: 125–132.
24. Zou, L., Y. Feng, Y. J. Chen, R. Si, S. Shen, Q. Zhou, F. Ichinose, M. Scherrer-Crosbie, and W. Chao. 2010. Toll-like receptor 2 plays a critical role in cardiac dysfunction during polymicrobial sepsis. *Crit. Care Med.* 38: 1335–1342.
25. Zou, L., Y. Feng, M. Zhang, Y. Li, and W. Chao. 2011. Nonhematopoietic toll-like receptor 2 contributes to neutrophil and cardiac function impairment during polymicrobial sepsis. *Shock* 36: 370–380.
26. Walker, W. E., A. T. Bozzi, and D. R. Goldstein. 2012. IRF3 contributes to sepsis pathogenesis in the mouse cecal ligation and puncture model. *J. Leukoc. Biol.* 92: 1261–1268.
27. Bergin, P. F., J. D. Doppelt, W. G. Hamilton, G. E. Mirick, A. E. Jones, S. Sritulanondha, J. M. Helm, and R. S. Tuan. 2010. Detection of periprosthetic infections with use of ribosomal RNA-based polymerase chain reaction. *J. Bone Joint Surg. Am.* 92: 654–663.
28. Pangburn, M. K., and H. J. Müller-Eberhard. 1984. The alternative pathway of complement. *Springer Semin. Immunopathol.* 7: 163–192.
29. Hotchkiss, R. S., K. W. Tinsley, P. E. Swanson, K. C. Chang, J. P. Cobb, T. G. Buchman, S. J. Korsmeyer, and I. E. Karl. 1999. Prevention of lymphocyte cell death in sepsis improves survival in mice. *Proc. Natl. Acad. Sci. USA* 96: 14541–14546.

Downloaded from http://journals.aai.org/jimmunol/article-pdf/196/6/2788/1417822/1502106.pdf by guest on 06 March 2025

30. Hotchkiss, R. S., K. W. Tinsley, and I. E. Karl. 2003. Role of apoptotic cell death in sepsis. *Scand. J. Infect. Dis.* 35: 585–592.
31. Angus, D. C., and T. van der Poll. 2013. Severe sepsis and septic shock. *N. Engl. J. Med.* 369: 2063.
32. Alexopoulou, L., A. C. Holt, R. Medzhitov, and R. A. Flavell. 2001. Recognition of double-stranded RNA and activation of NF-kappaB by Toll-like receptor 3. *Nature* 413: 732–738.
33. Lund, J. M., L. Alexopoulou, A. Sato, M. Karow, N. C. Adams, N. W. Gale, A. Iwasaki, and R. A. Flavell. 2004. Recognition of single-stranded RNA viruses by Toll-like receptor 7. *Proc. Natl. Acad. Sci. USA* 101: 5598–5603.
34. Crozat, K., and B. Beutler. 2004. TLR7: A new sensor of viral infection. *Proc. Natl. Acad. Sci. USA* 101: 6835–6836.
35. O'Neill, L. A., and A. G. Bowie. 2007. The family of five: TIR-domain-containing adaptors in Toll-like receptor signalling. *Nat. Rev. Immunol* 7: 353–364.
36. Karikó, K., H. Ni, J. Capodici, M. Lamphier, and D. Weissman. 2004. mRNA is an endogenous ligand for Toll-like receptor 3. *J. Biol. Chem.* 279: 12542–12550.
37. Bernard, J. J., C. Cowing-Zitron, T. Nakatsuji, B. Muehleisen, J. Muto, A. W. Borkowski, L. Martinez, E. L. Greidinger, B. D. Yu, and R. L. Gallo. 2012. Ultraviolet radiation damages self noncoding RNA and is detected by TLR3. *Nat. Med.* 18: 1286–1290.
38. Karikó, K., M. Buckstein, H. Ni, and D. Weissman. 2005. Suppression of RNA recognition by Toll-like receptors: the impact of nucleoside modification and the evolutionary origin of RNA. *Immunity* 23: 165–175.
39. Heil, F., H. Hemmi, H. Hochrein, F. Ampenberger, C. Kirschning, S. Akira, G. Lipford, H. Wagner, and S. Bauer. 2004. Species-specific recognition of single-stranded RNA via toll-like receptor 7 and 8. *Science* 303: 1526–1529.
40. Taganov, K. D., M. P. Boldin, K. J. Chang, and D. Baltimore. 2006. NF-kappaB-dependent induction of microRNA miR-146, an inhibitor targeted to signaling proteins of innate immune responses. *Proc. Natl. Acad. Sci. USA* 103: 12481–12486.
41. O'Neill, L. A., F. J. Sheedy, and C. E. McCoy. 2011. MicroRNAs: the fine-tuners of Toll-like receptor signalling. *Nat. Rev. Immunol.* 11: 163–175.
42. Nahid, M. A., M. Satoh, and E. K. Chan. 2011. MicroRNA in TLR signaling and endotoxin tolerance. *Cell. Mol. Immunol.* 8: 388–403.
43. Brudecki, L., D. A. Ferguson, C. E. McCall, and M. El Gazzar. 2013. MicroRNA-146a and RBM4 form a negative feed-forward loop that disrupts cytokine mRNA translation following TLR4 responses in human THP-1 monocytes. *Immunol. Cell Biol.* 91: 532–540.
44. El Gazzar, M., A. Church, T. Liu, and C. E. McCall. 2011. MicroRNA-146a regulates both transcription silencing and translation disruption of TNF-α during TLR4-induced gene reprogramming. *J. Leukoc. Biol.* 90: 509–519.
45. Cheng, H. S., N. Sivachandran, A. Lau, E. Boudreau, J. L. Zhao, D. Baltimore, P. Delgado-Olguin, M. I. Cybulsky, and J. E. Fish. 2013. MicroRNA-146 represses endothelial activation by inhibiting pro-inflammatory pathways. *EMBO Mol. Med.* 5: 949–966.
46. Gao, M., X. Wang, X. Zhang, T. Ha, H. Ma, L. Liu, J. H. Kalbfleisch, X. Gao, R. L. Kao, D. L. Williams, and C. Li. 2015. Attenuation of Cardiac Dysfunction in Polymicrobial Sepsis by MicroRNA-146a Is Mediated via Targeting of IRAK1 and TRAF6 Expression. *J. Immunol.* 195: 672–682.
47. Fabbri, M., A. Paone, F. Calore, R. Galli, E. Gaudio, R. Santhanam, F. Lovat, P. Fadda, C. Mao, G. J. Nuovo, et al. 2012. MicroRNAs bind to Toll-like receptors to induce prometastatic inflammatory response. *Proc. Natl. Acad. Sci. USA* 109: E2110–E2116.
48. Park, C. K., Z. Z. Xu, T. Berta, Q. Han, G. Chen, X. J. Liu, and R. R. Ji. 2014. Extracellular microRNAs activate nociceptor neurons to elicit pain via TLR7 and TRPA1. *Neuron* 82: 47–54.
49. Lehmann, S. M., C. Krüger, B. Park, K. Derkow, K. Rosenberger, J. Baumgart, T. Trimbuch, G. Eom, M. Hinz, D. Kaul, et al. 2012. An unconventional role for miRNA: let-7 activates Toll-like receptor 7 and causes neurodegeneration. *Nat. Neurosci.* 15: 827–835.
50. Pearson, G., F. Robinson, T. Beers Gibson, B. E. Xu, M. Karandikar, K. Berman, and M. H. Cobb. 2001. Mitogen-activated protein (MAP) kinase pathways: regulation and physiological functions. *Endocr. Rev.* 22: 153–183.
51. Chen, Z., T. B. Gibson, F. Robinson, L. Silvestro, G. Pearson, B. Xu, A. Wright, C. Vanderbilt, and M. H. Cobb. 2001. MAP kinases. *Chem. Rev.* 101: 2449–2476.
52. Arthur, J. S., and S. C. Ley. 2013. Mitogen-activated protein kinases in innate immunity. *Nat. Rev. Immunol.* 13: 679–692.

Downloaded from http://journals.aai.org/jimmunol/article-pdf/196/6/2788/1417822/1502106.pdf by guest on 06 March 2025